GEOPHYSICAL RESEARCH LETTERS, VOL. 27, NO. 18, PAGES 3005-3008, SEPTEMBER 15, 2000

Crustal shortening in the Andes: Why do GPS rates differ from geological rates?

Mian Liu[1], Youqing Yang[1], Seth Stein[2], Yuanqing Zhu[1] and Joe Engeln[1]

Abstract. GPS data indicate 30-40 mm yr^{-1} present-day crustal shortening across the Andes, whereas geological evidence shows crustal shortening concentrated in the sub-Andean thrust belt at a much lower rate (<15 mm yr^{-1}). We reconcile the discrepancy between the geodetic and the geological crustal shortening using geodynamic modeling that includes timescale-dependent crustal deformation. The GPS velocities reflect the instantaneous deformation in the Andes that includes both permanent deformation and elastic deformation that will be recovered during future earthquakes, whereas the lower geological rates reflect only the permanent deformation. The three-dimensional viscoelastic model predicts nearly uniform short-term velocity gradients across the Andes, similar to the GPS results, and concentrated long-term crustal shortening in the sub-Andean thrust zone, consistent with geological observations.

1. Introduction

One of the most satisfying validations for the theory of plate tectonics comes from GPS and other space geodetic methods. With precision to a few mm yr^{-1}, these geodetic measurements show that many parts of the Earth's surface move relative to each other very much as predicted by plate motion models derived from geological data spanning millions of years [*Stein*, 1993]. However, in the Andes, the crustal shortening inferred from short-term geodetic measurements differs significantly from that indicated by the geological record, suggesting that the crust may deform differently on different timescales. Here we use a simple plastic-viscoelastic model to illustrate the relationship between the instantaneous crustal shortening reflected in the GPS measurements and long-term crustal shortening indicated by geological observations. We then present a three-dimensional finite element model that incorporates digital topography and relevant model geometry and boundary conditions of the Andean orogen. The model predicts a nearly uniform short-term velocity gradient across the Andes consistent with the GPS data, and long-term crustal shortening concentrated in the sub-Andean thrust belt consistent with geological evidence.

2. The Andean Crustal Shortening

Although numerous factors, including magmatic addition and mantle flow, may have contributed to the Andean mountain building [*Fukao et al.*, 1989; *Russo and Silver*, 1996; *Zandt et al.*, 1996; *Pope and Willett*, 1998], most workers believe that the Andes resulted largely from crustal shortening in the past ~30 Myr as the consequence of convergence between the subducting Nazca plate and the overriding South American plate [*Isacks*, 1988; *Sheffels*, 1990; *Dewey and Lamb*, 1992]. The present crustal shortening associated with the plate convergence is clearly shown in recent GPS results spanning the Central Andes [*Leffler et al.*, 1997; *Norabuena et al.*, 1998] (Fig. 1). The GPS velocity of the Nazca plate is 68-78 mm yr^{-1} relative to the stable interior of the South America plate [*Norabuena et al.*, 1999], slightly less than the predictions of the NUVEL-1A plate motion model, which was based on marine magnetic anomalies averaged over the past 3 Myr [*DeMets et al.*, 1994]. About half of the plate convergence is locked at the plate boundary, causing 30-40 mm yr^{-1} eastward movement of the coastal area relative to stable South America (Fig. 1). The gradual decrease of GPS velocity across the Andes indicates crustal shortening in the entire mountain belt. The geological evidence, however, shows crustal shortening concentrated within the sub-Andean fold-and-thrust belt (FTB) at a much lower rate (8-13 mm yr^{-1})

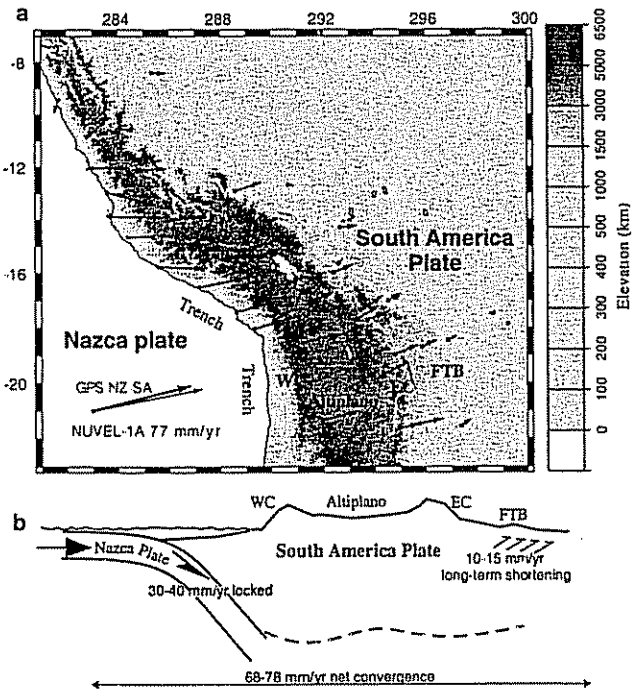

Figure 1. (a) Topography and GPS site velocity field relative to stable South America (SA) [*Leffler et al.*, 1997; *Norabuena et al.*, 1998] of the central Andes. Rate scale is given by the NUVEL-1A vector. NZ, Nazca plate; WC, Western Cordillera; EC, Eastern Cordillera; FTB, Sub-Andean Fold and Thrust belt. (b) Sketch of a cross-section of the Andean orogenic system showing velocity distribution inferred from GPS data.

[1] Dept. of Geological Sciences; University of Missouri, Columbia, MO, 65211
[2] Dept. of Geological Sciences, Northwestern University, Evanston, IL, 60208

Paper number 2000GL008532.
0094-8276/00/2000GL008532$05.00

averaged over the past 25 Myr [*Sheffels*, 1990; *Schmitz*, 1994]. Modern seismicity also shows active crustal shortening concentrated within the sub-Andean FTB. The shortening rate estimated from the seismic moments of earthquakes is only 1-3 mm yr^{-1} [*Suarez et al.*, 1983], which is a minimum because aseismic deformation is not included in the calculations and the sampling period may have missed infrequent very large earthquakes. The discrepancy between the geodetic and geological rates and spatial distributions of crustal shortening can be reconciled by the timescale-dependent behavior of the lithosphere, which behaves as an elastic body over a short period but as viscous flow over the geological timescale of millions of years.

3. Short-Term vs. Long-Term Crustal Shortening Rates

Transient strain accumulation and release associated with the seismic cycle at subduction zones have been well studied [*Savage*, 1983] Here we illustrate the relationships between the long-term and short-term behavior of crustal shortening across both the subduction zone and the Andes in a simple plastic-viscoelastic model containing a dashpot, a spring, and a pair of frictional plates (Fig. 2). The first two parts represent a viscoelastic body, and the frictional plates represents faults. This system provides a first-order approximation of the mechanical behavior of the Andean crust: mainly elastic over short periods, viscous over long geological time scales, and plastic (sliding along faults) when tectonic stresses exceed the yield strength of the crust. When the system is compressed at a constant rate V_o, which is 30 - 40 mm yr^{-1} at the leading edge of South America, the stress $\sigma(t)$ increases with time: $\sigma(t) = \sigma_m - (\sigma_m - \sigma_b)\exp(-t/\tau)$, where σ_b is the background stress, t is time, $\tau = \eta / E$ is the Maxwell relaxation time, and $\sigma_m = \eta V_o / W$ is the theoretical limit of stress in the system, where η is viscosity, E is the Young's modulus, and W is the width of the deforming zone. Fig. 2b shows the stress evolution in this model. Whenever stress reaches the yield strength, sliding (an earthquake) occurs between the frictional plates, stress drops to σ_b, and the process then repeats. The resultant displacement evolution shows the relation between short-term strain and long-term permanent shortening (Fig. 2c). Correlating to the stress evolution, displacement accumulates at the rate of V_o except during earthquakes, when it drops by an amount Δu. The averaged long-term shortening rate at the compressional edge of the system, V_c, is given by V_o minus the average slip rate, as shown by the envelope of the displacement sawtooth-curve (Fig. 2c). This relationship explains why the GPS-measured crustal shortening rates are higher than the geologically-derived shortening rates. The long-term shortening rate V_c can be simplified as $V_c = W\sigma_y / \eta$. When the shortening is uniformly distributed across the system, V_c / W is the strain rate: $V_c / W = \dot{\varepsilon} = \sigma_y / \eta$ In other words, the averaged long-term deformation of this plastic-viscoelastic system is essentially that of a viscous fluid.

4. Uniform Shortening vs. Concentrated Shortening

To understand why the geodetically measured crustal shortening is essentially smoothly distributed across the entire Andean mountain belt whereas the geological evidence indicates concentrated crustal shortening in the sub-Andean FTB, we examine the Andean geodynamic system and its three-dimensional boundary conditions. The major driving force is tectonic compression associated with the continued plate convergence, which is largely balanced by the gravitational buoyancy force arising from the isostatically supported elevation of the mountain ranges [*Dalmayrac and Molnar*, 1981; *Molnar and Lyon-Caen*, 1988]. The former acts to build the mountains, while the later tends to collapse the mountains. We simulate the Andean crustal deformation using three-dimensional finite element modeling (Fig. 3). The lateral boundary conditions are specified by velocity boundary conditions consistent with the GPS measurements (see Fig. 1): a displacement boundary along the western edge of the model, a roller condition on the northern and southern boundaries to restrict displacement to the direction of plate convergence, and a roller condition along the eastern side reflecting no crustal shortening within stable South America. The gravitational buoyancy force is calculated using the digital topography of the Andes, assuming a crustal density

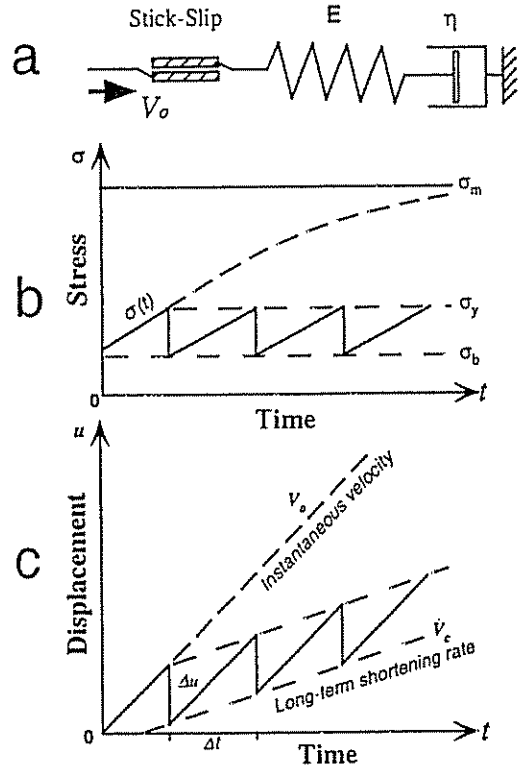

Figure 2. (a) Analog model for a plastic-viscoelastic crust. The frictional plates model the effects of earthquake cycle at the trench, the dashpot models viscous flow leading to permanent deformation, and the spring models elastic deformation that will be recovered by earthquakes (sliding of the frictional plates). (b) Stress evolution for the viscoelastic-plastic system. Symbols are explained in text. (c) Displacement evolution showing the relationship between instantaneous velocity and long-term permanent velocity at the left end of the viscoelastic-plastic system. Displacement accumulates at the instantaneous rate V_o except during sliding (earthquake) events, when a rebound Δu occurs. Hence GPS data would record a gradient starting at V_o from the trench, whereas the envelope of the displacement curve V_c is the long-term shortening rate reflected in geological records.

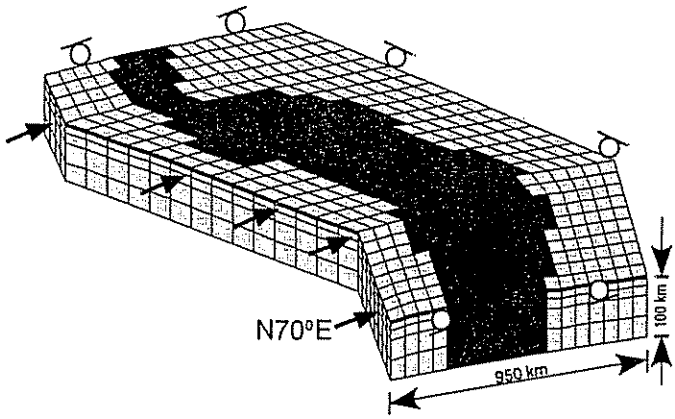

Figure 3. Finite element mesh and boundary conditions. Dark areas are the Andean mountain belt. Digital topography of the Andes is used for calculating the gravitational body force. The model has six layers with variable viscosity approximating the typical strength profile of the lithosphere.

of 2800 kg m^{-3}. The elastic parameters used in the calculations include the Young's modulus ($7x10^{10}$ MPa) and the Poisson's ratio (0.25). Winkler springs are used to simulate the body forces induced by vertical displacement of density boundaries and the isostatic restoring force at the base of the model crust [*Williams and Richardson*, 1991]. The model lithosphere is 100 km thick and has six layers with variable effective viscosity to approximate the typical strength profile of the continental lithosphere [*Kirby and Kronenberg*, 1987]. For each layer, the viscosity under the mountain belt is assumed to be one order of magnitude lower than that under the lowlands.

At a short time scale ($<10^2$ yr) crustal deformation is expected to be near-elastic, which is approximated with high viscosity (10^{25}-10^{27} Pa s) for the various crustal layers (Fig. 4a). A velocity boundary condition ranging from 32 - 35 mm yr^{-1} with respect to stable South America was imposed on the western side of the model. The small variations of velocity on this boundary result from scaling with the model width, a procedure used to avoid introducing artificial internal distortion because of the simplified model geometry. The results show a nearly uniform decrease of velocity from the west across the entire mountain belt, consistent with the GPS-based velocity field (cf. Fig. 1).

Over long geological time scales ($>10^6$ yr), the observed crustal deformation is similar to that predicted for a viscous fluid [*England and McKenzie*, 1982] with an average effective

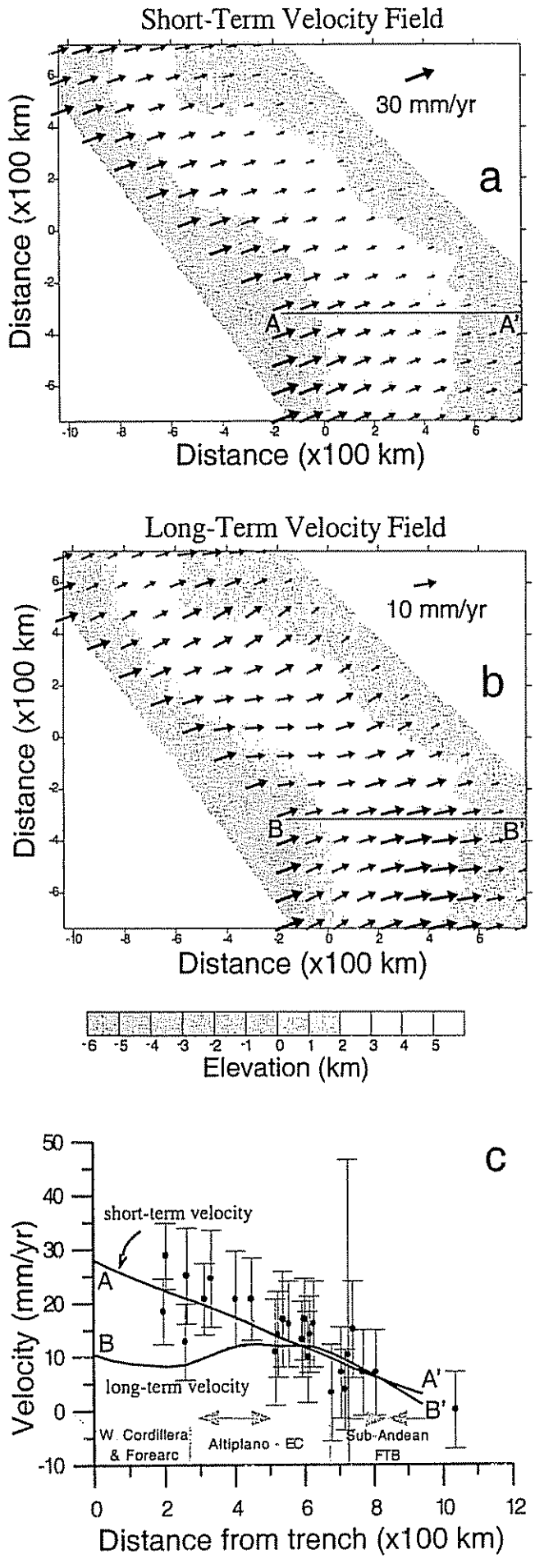

Figure 4. (a) Predicted velocities across the Andes for short-term crustal deformation. Scale is shown in the upper right corner. Solid line (A-A') indicates the location of the velocity profile in (c). (b) Predicted velocities for long-term crustal deformation. The non-uniform velocity gradients across the Andes are caused by gravitational spreading superimposed on the deformation resulting from tectonic compression along the western boundaries. Solid line (B-B') indicates the location of velocity profile in (c). (c) Comparison of the predicted short-term and long-term crustal deformation across the Andes with GPS velocity data [*Norabuena et al*, 1998]. The pairs of arrows show E-W compressional (convergent) or extensional (divergent) stress states inferred from the velocity gradients for long-term deformation.

viscosity between 10^{22} and 10^{24} Pa s [*England and Houseman*, 1986]. To simulate the long-term crustal shortening in the Andes, we lower the viscosity of crust layers to 10^{22}-10^{23} Pa s in the model (Fig. 4b). A velocity boundary condition of 10-12 mm yr^{-1} is applied to the west side of the model, as suggested by the geologically averaged shortening rates [*Sheffels*, 1990; *Schmitz*, 1994]. The resultant velocity field shows significantly non-uniform gradients across the Andes, in contrast to short-term crustal deformation (Fig. 4c). This difference is caused by gravitational spreading of the mountain belt, which is negligible for short-term (high effective viscosity) deformation but becomes important over the long geological time scales (low effective viscosity). While crustal shortening associated with plate convergence pushes the crustal material eastward, gravitational spreading moves the crustal material to both sides of the mountain belt. Over the Eastern Cordillera and part of the Altiplano, the eastward velocity due to compression at the plate boundary is amplified by gravitational spreading in the same direction, causing the velocity peak over this region (Fig. 4c). This is clearer in regions south of the bend at 22°S where the mountain ranges are higher and wider, enhancing the effects of gravitational spreading. The high velocity gradient across the sub-Andean zone indicates concentrated crustal shortening, consistent with geological and seismological observations. The long-term velocity in the Western Cordillera is relatively low, because there gravitational spreading is in the direction opposite (westward) of the eastward tectonic compression. The predicted topography and long-term stress patterns in central Andes are also comparable to the observations [*Liu et al.*, 1999].

The model velocity field is largely controlled by the viscosity structure. We find the short-term shortening across the Andes as reflected by the GPS data can be reasonably well fit when the viscosity of the model crust is $>10^{24}$ Pa s. The boundary conditions and the force balance between tectonic compression and gravitational spreading are also important for the predicted velocity, the effects of other model simplifications are secondary.

5. Discussion

The uncertainties of present GPS data are large enough to allow alternative (nonuniform) interpretations of the velocity field [*Leffler et al.*, 1997; *Norabuena et al.*, 1998]. A longer interval of measurements would reduce the uncertainties sufficiently to resolve this issue. Nonetheless, the significant discrepancies between GPS and geological rates and distribution of crustal shortening in the Andes would remain and be consistent with the general model proposed here. The timescale-dependent mechanical behavior of continental crust may explain discrepancies between GPS and geological rates at different tectonic settings. For example, within some diffusive deformation zones, the geological rates may include both aseismic and seismic slips. Thus GPS rates measured within an earthquake cycle could be lower than geological rates averaged over a longer time interval [*Larson et al.*, 1999]. As increasingly more space geodetic data are being acquired and integrated with other data for plate boundary zones around the world, models like those presented here should be useful for understanding crustal deformation in other regions.

Acknowledgments. We thank W. Holt and D. Argus for constructive review, and T. Dixon and E. Klosko for helpful discussions. This work was supported by NSF grant EAR-9805127 and NASA grant NAG5-9145.

References

Dalmayrac, B., and P. Molnar, Parallel thrust and normal faulting in Peru and constrains on the state of stress, *Earth Planet. Sci. Lett.*, *55*, 473-481, 1981.

DeMets, C., R.G. Gordon, D.F. Argus, and S. Stein, Effect of recent revisions to the geomagnetic reversal time scale on estimates of current plate motion, *Geophys. Res. Lett.*, *21*, 2191-2194, 1994.

Dewey, J.F., and S.H. Lamb, Active tectonics of the Andes, *Tectonophysics*, *205*, 79-95, 1992.

England, P.C., and G.A. Houseman, Finite strain calculations of continental deformation 2. Comparison with the India-Asia collision, *J. Geophys. Res.*, *91*, 3664-3676, 1986.

England, P.C., and D.P. McKenzie, A thin viscous sheet model for continental deformation, *Geophys. J. R. astr. Soc*, *70*, 295-321, 1982.

Fukao, Y., A. Yamamoto, and M. Kono, Gravity anomaly across the Peruvian Andes, *J. Geophys. Res.*, *94*, 3867-3890, 1989.

Isacks, B.L., Uplift of the central Andean plateau and bending of the Bolivian orocline, *J. Geophys Res*, *93*, 3211-3231, 1988.

Kirby, S.H., and A.K. Kronenberg, Rheology of the lithosphere: Selected topics, *Rev Geophys*, *25*, 1,219-1,244, 1987.

Larson, K., R. Burgmann, R. Bilham, and J.T. Freymueller, Kinematics of the India-Eurasia collision zone from GPS measurements, *J. Geophys Res*, *104*, 1077-1094, 1999.

Leffler, L., S. Stein, A. Mao, T. Dixon, M. Ellis, L. Ocala, and I.S. Sacks, Constraints on the present-day shortening rate across the Central Eastern Andes from GPS measurements, *Geophys. Res. Lett.*, *24*, 1031-1034, 1997.

Liu, M., Y. Yang, Y. Zhu, S. Stein, and E. Klosko, Crustal extension in the Andes and the Tibetan lateau: Insight from 3D finite element modeling, *EOS, Trans. AGU*, *80*, F1061, 1999.

Molnar, P., and H. Lyon-Caen, Some simple physical aspects of the support, structure, and evolution of mountain belts, *Geol. Soc. Ame. Spec. Pap.*, *218*, 179-207, 1988.

Norabuena, E., L. Leffler-Griffin, A. Mao, T. Dixon, S. Stein, I.S. Sacks, L. Ocala, and M. Ellis, Space geodetic observations of Nazca-South America convergence along the Central Andes, *Science*, *279*, 358-362, 1998.

Norabuena, E.O., T.H. Dixon, S. Stein, and C.G.A. Harrison, Decelerating Nazca-South America and Nazca-Pacific plate motions, *Geophys. Res. Lett.*, *26*, 3405-3408, 1999.

Pope, D.C., and S.D. Willett, Thermal-mechanical model for crustal thickening in the central Andes driven by ablative subduction, *Geology*, *26*, 511-514, 1998.

Russo, R.M., and P.G. Silver, Cordillera formation, mantle dynamics, and the Wilson cycle, *Geology*, *24*, 511-514, 1996.

Savage, J.C., A dislocation model of strain accumulation and release at a subduction zone, *J. Geophys. Res.*, *88*, 4984-4996, 1983.

Schmitz, M., A balanced model of the southern Central Andes, *Tectonics*, *13*, 484-492, 1994.

Sheffels, B., Lower bound on the amount of crustal shortening in the central Bolivian Andes, *Geology*, *18*, 812-815, 1990.

Stein, S., Space geodesy and plate motions, in *Space Geodesy and Geodynamics*, edited by D.E. Smith, and D.L. Turcotte, pp. 5-20, American Geophysical Union, Washington, D.C., 1993.

Suarez, G., P. Molnar, and B.C. Burchfiel, Seismicity, fault plane solutions, depth of faulting, and active tectonics of the Andes of Peru, Ecuador, and southern Colombia, *J. Geophys. Res.*, *88*, 10403-10428, 1983.

Williams, C.A., and R.M. Richardson, A rheological layered three-dimensional model of the San Andreas Fault in central and southern California, *J. Geophys. Res.*, *96*, 16597-16623, 1991.

Zandt, G., S.L. Beck, S.R. Ruppert, C.J. Ammon, D. Rock, E. Minaya, T.C. Wallace, and P.G. Silver, Anomalous crust of the Bolivian Altiplano, Central Andes: constraints from broadband regional seismic waveforms, *Geophys. Res. Lett.*, *23*, 1159-1162, 1996.

Mian Liu, Youqing Yang, Yuanqing Zhu and Joe Engeln, Dept. of Geological Sciences, University of Missouri, Columbia, MO 65211 (Email: liu m@missouri.edu)

Seth Stein, Dept. of Geological Sciences, Northwestern University, Evanston, IL, 60208

(Received March 27, 2000; revised June 30, 2000; accepted August 1, 2000.)